J. Membrane Biol. 130, 1–10 (1992)

The Journal of
Membrane Biology

A Naphthyl Analog of the Aminostyryl Pyridinium Class of Potentiometric Membrane Dyes Shows Consistent Sensitivity in a Variety of Tissue, Cell, and Model Membrane Preparations

Leslie M. Loew†‡*, Lawrence B. Cohen§, James Dix‡, Eric N. Fluhler‡**, Valerie Montana†, Guy Salama¶, and Wu Jian-young§

†Department of Physiology, University of Connecticut Health Center, Farmington, Connecticut 06030, §Department of Physiology, Yale University School of Medicine, New Haven, Connecticut 06510, §Marine Biological Laboratory, Woods Hole, Massachusetts 02543, ‡Department of Chemistry, State University of New York at Binghamton, Binghamton, New York 13901, ¶Department of Physiology, University of Pittsburgh School of Medicine, Pittsburgh, Pennsylvania

Summary. The fast potentiometric indicator di-4-ANEPPS is examined in four different preparations: lipid vesicles, red blood cells, squid giant axon, and guinea pig heart. The dye gives consistent potentiometric responses in each of these systems, although some of the detailed behavior varies. In lipid vesicles, the dye displays an increase in fluorescence combined with a red shift of the excitation spectrum upon hyperpolarization. Similar behavior is found in red cells where a dual wavelength ratiometric measurement is also demonstrated. The signal-to-noise ratio of the potentiometric fluorescence response is among the best ever recorded on the voltage-clamped squid axon. The dye is shown to be a faithful and persistent monitor of cardiac action potentials with no appreciable loss of signal or deterioration of cardiac activity for periods as long as 2 hr with intermittent illumination every 10 min. These results, together with previously published applications of the dye to a spherical lipid bilayer model and to cells in culture, demonstrate the versatility of di-4-ANEPPS as a fast indicator of membrane potential.

Key Words potential-sensitive dyes · red blood cells · squid axon · fluorescence spectroscopy · heart · membrane potential

Introduction

Over the last 15 years a large number of dyes have been screened for fast potential-dependent optical signals capable of monitoring voltage changes across the membranes of excitable cells (Cohen et al., 1974; Ross et al., 1977; Gupta et al., 1981). Members of various structural classes of dyes have proven successful in different applications (for a series of reviews *see* Loew, 1988). The class of "styryl" dyes, which usually contain a *p*-dialkyaniline linked to the 4- position of a pyridinium nucleus via one or more double bonds, has provided a number of sensitive fluorescent probes of membrane potential (Loew & Simpson, 1981; Grinvald et al., 1982; Grinvald et al., 1983; Fluhler et al., 1985). A theoretical study of these chromophores (Loew, Bonneville & Surow, 1978) indicated that they undergo a large charge shift upon excitation. Thus, a properly oriented styryl dye might be expected to display an electrochromic (Platt, 1956) response to membrane potential. Indeed, the results of studies on a spherical lipid bilayer model membrane system were compatible with this mechanism (Loew et al., 1979; Loew & Simpson, 1981; Fluhler et al., 1985). On the other hand, not all the styryl dyes displayed exclusively electrochromic behavior in other membrane systems (Loew et al., 1985); it appears that differing membrane environments can bring other mechanisms to the fore which can mask or swamp out any underlying electrochromic response. In general, it has been found that neither sensitivity nor mechanism is conserved as a given probe is applied to different cells or tissue preparations (Ross & Reichardt, 1979). The largest voltage-dependent fluorescence change, 21%/100 mV, has been reported in a neuroblastoma cell for the styryl dye RH421 (Grinvald et al., 1983).

A styryl dye, di-4-ANEPPS, in which the aniline is replaced with a dialkylaminonaphthalene moiety, displays the largest fractional fluorescence response on the spherical bilayer of any of the charge shift probes tested (Fluhler et al., 1985). The wavelength dependence of the transmittance and fluorescence changes indicate simple shifts of the absorption, excitation and emission spectra—as would be predicted for electrochromism. It has been used to de-

* *Correspondence address:* To L.M.L. at the University of Connecticut Health Center.

** *Present address:* Pharmacology Department, RJR-Nabisco, Winston Salem, North Carolina 27102.

termine electric field-induced membrane potential in a number of different cell types (Gross et al., 1986*a*, *b*; Ehrenberg et al., 1987). It has also recently been used to demonstrate the applicability of a dual wavelength ratiometric approach in measurements of membrane potential (Montana, Farkas & Loew, 1989).

In this paper, we evaluate di-4-ANEPPS in a series of four very different preparations: lipid vesicles with valinomycin-mediated K^+ diffusion potentials; voltage-clamped squid giant axon; red blood cell suspensions; and electrically active cardiac tissue. In earlier work (Gross et al., 1986*a*, *b*; Ehrenberg et al., 1987), di-4-ANEPPS was used to measure electric field-induced membrane potential on several different tissue culture cell types. The dye is quite successful at monitoring rapid potential changes and, in those cases where a valid comparison can be made, with about the same sensitivity as displayed in the voltage-clamped spherical bilayer—a relative fluorescence change of ~10%/100 mV (Fluhler et al., 1985). Interestingly, the electrochromic mechanism is not always the dominant source of this response but may often be extracted via a dual-wavelength ratio measurement.

Materials and Methods

Lipid Vesicles

Solutions were buffered with HEPES/tris pH 7.0 and contained either 100 mM, K_2SO_4 (high K buffer) or 300 mM sucrose and 1 mM K_2SO_4 (low K buffer). Lipid vesicles were prepared by sonicating 20 mg of egg phosphatidyl choline (Sigma, St. Louis, MO; Type XI-E) with 1 ml of the appropriate buffer under argon to clarity using a cylindrical bath sonicator (Laboratory Supplies, Hicksville, NY). A 30 μl aliquot of vesicle suspension was diluted into 3 ml of buffer containing 0.5 μM di-4-ANEPPS (Hassner et al., 1984). The ratio of the high and low K buffers was varied to set different concentration gradients across the vesicle membrane. Upon addition of 1.8 μM valinomycin (Aldrich, Milwaukee, WI), a K^+ diffusion potential, V, is generated as given by the Nernst equation:

$$V = -RT/n([K^+]_{in}/[K^+]_{out}).$$

The fluorescence of the vesicle suspension was measured with a SPEX CM dual wavelength fluorescence spectrometer (SPEX Industries, Edison, NJ). Conventional corrected emission or excitation spectra can be obtained with this instrument, which also has the ability to monitor emission excited from two excitation monochromators; excitation is rapidly alternated between the two excitation wavelengths via a 400 Hz chopper.

Perfused Heart

Guinea pigs were anesthetized with Nembutol (30 mg/kg), the hearts excised rapidly and perfused in a Langendorff apparatus with Krebs-Ringer's solution containing (in mM): NaCl 130, $NaHCO_3$ 12.5, $MgSO_4$ 1.2, KCl 4.75, dextrose 5, and $CaCl_2$ 2.5, at 34°C. The solution was gassed with 95% O_2 + 5% CO_2, setting the pH at 7.4. The temperature was monitored continuously and controlled to ± 0.2°C. Hearts were stained with the voltage-sensitive dye by perfusing the coronary vessels with 10 μM di-4-ANEPPS for 5 min by recycling 40 ml of perfusate containing dye. After the staining period, hearts were perfused with dye-free solutions for the rest of the experiment. The preparations were placed in a chamber with a front window to detect backward fluorescence emission from the dye bound to the cardiac cells. Epi-illumination was accomplished with a tungsten halogen lamp through a 50 mm f/1.8 Nikon lens. A 3 × 3, 6 × 6, or a 12 × 12 mm region of the heart's surface was focused on a 12 × 12 photodiode array such that each pixel on the array can record fluorescence changes from a well-defined region of the myocardium, 0.25 × 0.25, 0.5 × 0.5, or 1.0 × 1.0 mm, respectively. The depth-of-field of the optics was 125 μm so that cells 200 μm below the surface made a negligible contribution to the optical action potential signals. The interface between the array and the computer, and more detailed descriptions of the chamber and optics have been previously reported (Salama et al., 1987).

In the present experiments, simultaneous recordings of action potentials by optical and intracellular electrode techniques were obtained by dissecting the right ventricular free wall and pinning the sheet of muscle horizontally in a Sylguard-coated chamber. With the intact heart cannulated at the aorta, the left ventricle and septum were dissected while maintaining coronary perfusion to the right ventricular free wall. The left circumflex and anterior descending arteries were ligated to increase coronary perfusion pressure to the right ventricular wall and thus oxygenate the tissue through its coronary vasculature. Such capillary perfusion made it possible to record electrical activity from thick sheets of muscle (1 to 2 mm) without the expected hypoxia associated with limited diffusion of oxygen to the center of the tissue. A bipolar EKG electrode was placed at the base of the right ventricular sheet, just above the field of view of the array. The EKG electrode was made from 2 Ag/AgCl teflon-coated wires (100 μm in diameter) kept 0.5 mm apart by a rubber spacer. A microelectrode impaled a cardiac cell viewed by diode number 50, located at the edge of the field-of-view of the array. The electrode and diode signals were sampled simultaneously by the multiplexed analog-to-digital converters of the computer interface.

Red Blood Cells

Human blood less than three days old was obtained from the Binghamton, NY chapter of the American Red Cross. The blood was drawn into 5 ml tubes, with EDTA added as an anti-coagulant. Blood samples were centrifuged for 5 minutes at 3,000 × g after which the plasma and buffy coat were aspirated and discarded. The cells were then washed 3-5 times with 145 mM NaCl, 5 mM KCl, and 5 mM HEPES (N-2-hydroxyethylpiperazine-N'-2-ethanesulfonic acid), at pH 7.4 and resuspended to 50% hematocrit.

Steady-state fluorescence measurements of red cell suspensions containing potential sensitive probes were performed using a SLM instruments 8000 spectrofluorometer (Urbana, IL) or a SPEX CM System (Edison, NJ). Acrylic-sprayed stir bars and 3 ml acrylic cuvettes were used in all experiments in order to minimize dye binding. The resulting fluorescence data were sent to a MINC PDP 11/23 computer (Digital, Maynard, MA) for storage on disk and subsequent analysis.

Stopped-flow experiments were performed on a Dionex Model D-110 (Sunnyvale, CA) stopped-flow apparatus having a

dead time of 2 msec. The excitation source was a 150-watt xenon arc lamp (Oriel, Stratford, CT). An Oriel single monochromator was used to select the wavelength of light focused onto a fused silica fiber optic cable (also from Oriel). Output from the fiber optic cable was placed directly on the observation cell in the stopped-flow apparatus. Fluorescence was collected at 90° with a photomultiplier tube. Fluorescence emission was measured by placing appropriate high-pass filters between the observation chamber and the photomultiplier tube.

Squid Axon

A description of the apparatus for screening potentiometric dyes on the voltage-clamped squid axon has been published (Cohen et al., 1974; Ross et al., 1977; Gupta et al., 1981). The axon was stained with a saturated solution (< 20 μM) of di-4-ANEPPS in seawater for 10 min; the axon chamber was then flushed with several volumes of fresh dye-free argon-bubbled seawater before the start of the experiment.

Results

Squid Axon

Large absorbance and fluorescence responses were evident for di-4-ANEPPS applied externally to the voltage-clamped axon. A record of an experiment is shown in Fig. 1 indicating that the dye is potentiometric (the distortions in the optical traces during depolarizing voltage-clamp steps are artifacts from series resistance and imperfect space clamp as described by Davila et al., 1974). The potentiometric transmitted light response is shown as a function of wavelength in Fig. 2. The biphasic shape of this response spectrum is reminiscent of the spherical lipid bilayer (SB) spectrum (Fluhler et al., 1985). On the other hand, the dependence of the fluorescence change on excitation wavelength is not biphasic. This is at least partially due to the use of a high-pass cut-on filter in the emission path in this experiment, as necessitated by signal to noise considerations; the range of emission wavelengths selected by this filter corresponds to a region of net positive change in the emission wavelength dependent responses recorded on the SB (Fluhler et al., 1985). In other words, the excitation wavelength dependent changes shown in Fig. 2 actually contain a constant positive offset from the voltage-dependent change in the emission spectrum. The SB excitation response spectrum described by Fluhler et al. (1985), which is biphasic, is recorded by using an interference filter with a bandpass centered at the 0 crossover wavelength of the emission response.

The relative fluorescence changes are not very meaningful in the squid axon preparation because of the large background fluorescence associated with stained Schwann and connective tissue cells that cannot be completely dissected away (Gupta et al., 1981). The signal-to-noise ratio has been used as a quantitative figure of merit permitting comparison of the *ca.* 1200 dyes tested on the axon (Cohen et al., 1974; Ross et al., 1977; Gupta et al., 1981). It depends on instrumental details such as measurement bandwidth as well as the level of staining, persistence, extinction coefficient and fluorescence quantum yield of a dye in addition to the actual spectral sensitivity to membrane potential. With a bandwidth of 10-1000 Hz, di-4-ANEPPS has a signal-to-noise ratio of 9 in fluorescence and 11 in absorbance—comparable to the best of the styryl dyes.

Lipid Vesicles

The fluorescence response of di-4-ANEPPS bound to lipid vesicle membranes does not have a simple biphasic wavelength dependence. Figure 3 shows excitation and emission spectra obtained before and after development of a valinomycin mediated K^+ diffusion potential. Hyperpolarization clearly induces an increase in fluorescence intensity at all wavelengths along with a small red shift which is most easily appreciated by observing the relative positions of the wings of the spectra. Superimposed on the pure voltage-dependent change in these spectra is a small (<1%) increase due to an interaction of the dye with valinomycin. After correction for this effect, the relative fluorescence change can be obtained as a function of wavelength (Fig. 4), which also serves to accentuate the red shift. The curves in Fig. 4 can be interpreted to indicate a wavelength shift (from the sinusoidal shape reminiscent of the SB results) superimposed on an increase in total fluorescence upon hyperpolarization. The first-order electrochromic mechanism which has fit all the data on the SB, requires a biphasic wavelength dependence. Thus, the mechanism of the response on lipid vesicles may be a combination of electrochromism and at least one other process which changes the total fluorescence quantum yield.

Figure 5 shows the dependence on membrane potential at the combination of excitation and emission wavelengths which gives the best fractional change in fluorescence. The slope, 9.6%–100 mV, is similar to the calibration on SB. Also shown in this figure are data from experiments designed to determine if the potential-dependent fluorescence change is sensitive to dye concentration. The fractional fluorescence change varies insignificantly over two decades of dye concentration. At the highest of these concentrations the lipid to dye ratio is 25 : 1.

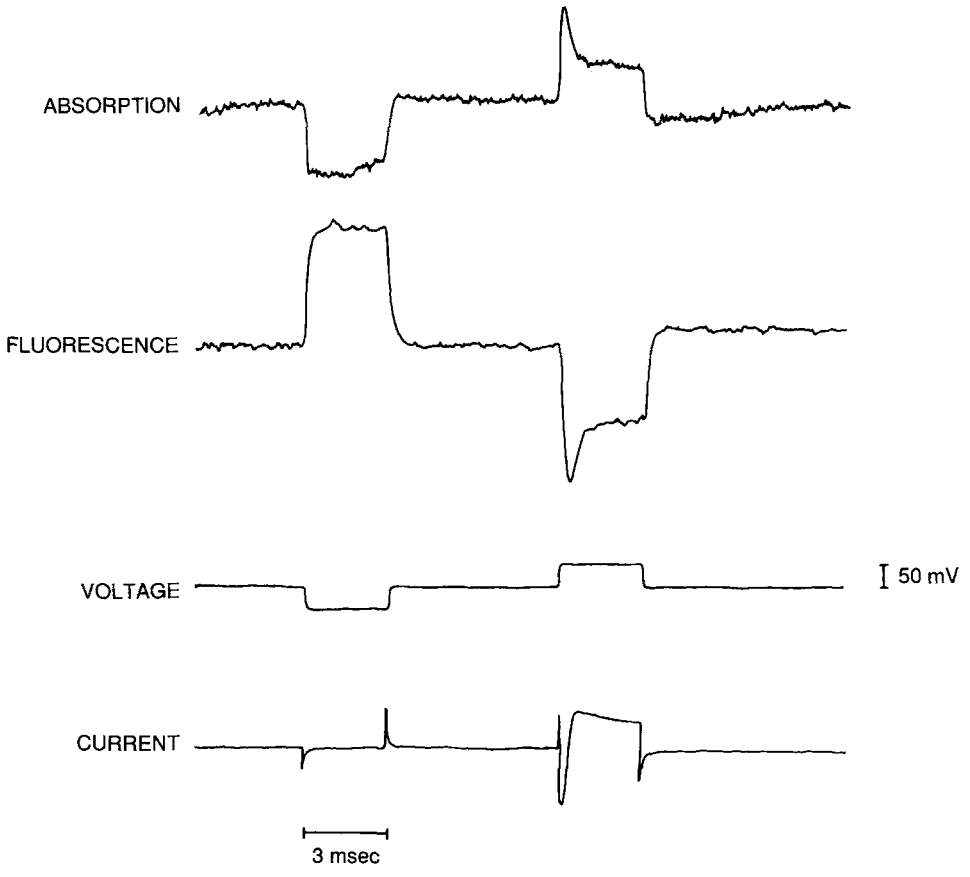

Fig. 1. Simultaneous absorption (top trace) and fluorescence (second trace) measurements from a squid giant axon stained with di-4-ANEPPS during 10 mV hyperpolarizing and depolarizing voltage clamp steps (third trace). The ionic currents are shown on the bottom trace. During the hyperpolarizing steps, on the left, the absorption and fluorescence changes had time courses which were similar to the time courses of the change measured by the voltage electrodes. During the depolarizing step, on the right, the distortion in the optical signals can be explained as resulting from the lack of compensation for resistance in series with the membrane and from an imperfect space clamp (Davila et al., 1974). The axon was stained with a 20 μM sea water solution of the dye for 10 min. A single pole high-frequency cut-off filter with a time constant of 60 μsec was used for the absorption measurements. The time constant for the fluorescence measurement was 170 μsec. The measurements were carried out at room temperature; 16 trials were averaged.

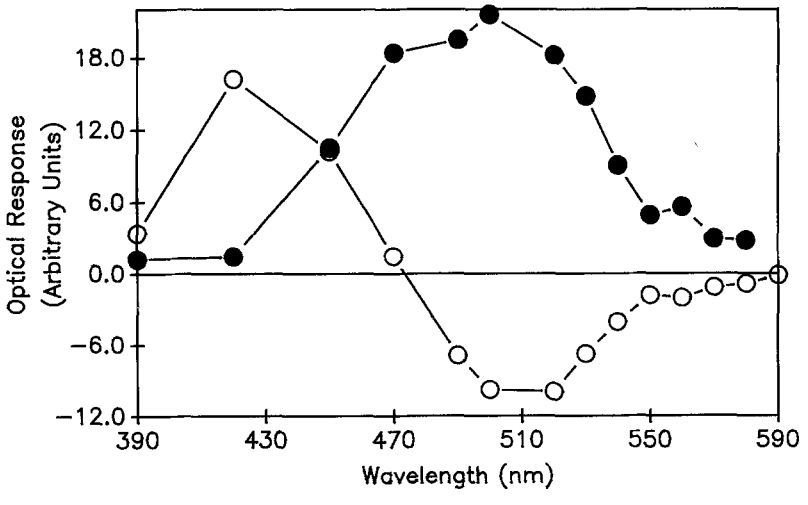

Fig. 2. Wavelength dependence of the spectral response of di-4-ANEPPS on the voltage-clamped squid giant axon. Open circles correspond to the transmittance change; filled circles are changes in the fluorescence emission as a function of excitation wavelength. Wavelengths of the incident light were selected with 10 nm bandpass interference filters. The emission was isolated from scattered light with a 590 nm longpass filter placed in front of the detector at 90° to the excitation. The changes measured are responses to 50 mV hyperpolarizing pulses.

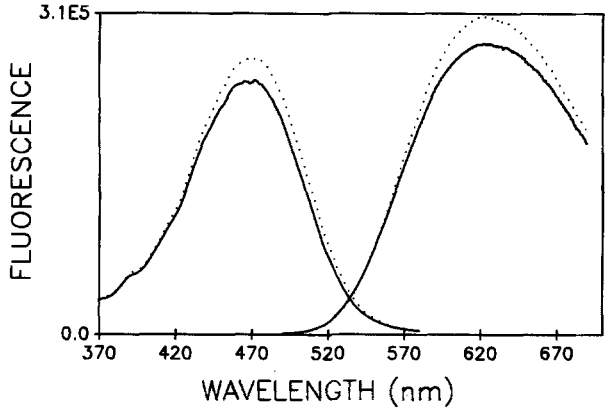

Fig. 3. Fluorescence excitation and emission spectra of di-4-ANEPPS bound to lipid vesicles before (solid curves) and after (dotted curves) −120 mV hyperpolarization. Lipid vesicles were prepared in 100 mM K_2SO_4 and diluted 100-fold into 300 mM sucrose containing 0.5 μM di-4-ANEPPS; the lipid concentration in the cuvette was 0.2 mg/ml. Solid and dotted spectra were obtained before and after, respectively, addition of 1.8 μM valinomycin. The excitation spectra on the left were obtained with the emission monochromator set at 610 nm; the emission spectra on the right were obtained with the excitation monochromator set at 472 nm.

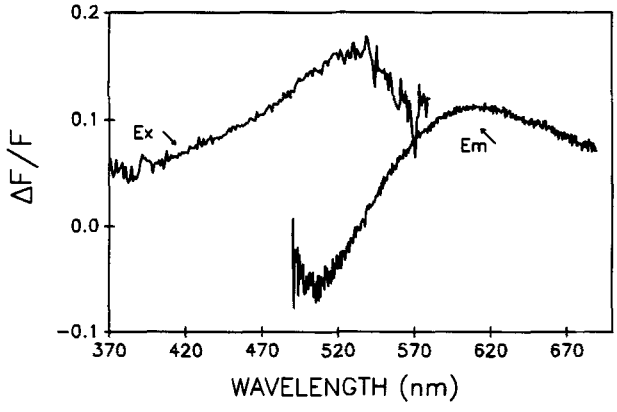

Fig. 4. Fractional fluorescence changes in response to a −120 mV hyperpolarization vs. excitation and emission wavelength. The excitation response spectrum on the left was generated by subtracting the resting excitation spectrum from the hyperpolarized excitation spectrum in Fig. 3 and dividing this difference by the resting spectrum. A similar set of operations was employed to generate the emission response spectrum.

Perfused Heart

Di-4-ANEPPS was found to be a sensitive and stable probe in various heart preparations such as working hearts (i.e., performing mechanical work), Langendorff isolated and perfused sheets of myocardium. The following experiment was designed to show the correlation of optical and microelectrode recording on an isolated, perfused sheet of guinea pig right ventricle. Microelectrode impalements could not be practically obtained on a Langendorff perfused heart. Consequently, an isolated, perfused right ventricular wall was pinned down horizontally, impaled with a microelectrode and imaged onto a 12 × 12 photodiode array to simultaneously record fluorescence signals. In Fig. 6, optical traces from diodes nos. 1, 68, 50, and 107 are shown simultaneously with the EKG and intracellular recording from a cell viewed by diode no. 50. The dye fluorescence monitored cardiac action potential with high fidelity with sharp upstrokes, elevated plateau phases and durations in the range of 200 msec. The time course of such optical action potentials indicated that the tissue was "healthy." The dye fluorescence was uniform across the surface of the tissue and the average fractional decrease of fluorescence relative to background was $-5.13 \pm 0.2\%$ ($n = 6$) per action potential (*ca.* −85 mV). The latter suggested that perfusion with dye solution resulted in homogeneously stained hearts. The excitation and emission wavelengths were 520 ± 20 nm and > 640 nm. By adding the relative changes at these wavelengths in the spherical bilayer response spectra (Fluhler et al., 1985), and adjusting for the difference in applied potential, it is demonstrated that the sensitivity is nearly identical.

The activation time point at each diode was defined as the time for maximum dF/dt at each diode (i.e., the time point at which most of the cells viewed by a photodiode were depolarizing) and was calculated for each action potential. The first diode(s) to activate were assigned an activation time point of 0.0 msec and all other activation time points were measured (in msec) relative to this. From the activation time delays, a grey scale isochronal map was generated to follow the firing sequence of action potential propagating across the surface of the tissue viewed by the array (Fig. 7). The location of the diode traces shown in Fig. 6 were labeled on the activation map, along with sites for intracellular (diode no. 50) and extracellular (EKG) recordings. Action potentials were initiated at the stimulus site (2 Hz), near the apex and swept diagonally across the tissue towards the base in 33.8 msec. The wavefront propagated (light to dark regions) along a direction perpendicular to the longitudinal fiber axis with a conduction velocity of 0.36 m/sec. Thus, the dye and the array made it possible to follow the rapid spread of electrical activity from a complex electrical syncitium.

The signals in Fig. 7 were recorded 10 min after perfusion with dye-free solution and were stable for over 2 hr during which recordings (i.e. continuous illumination of the preparation for 1-5 min) were taken every 10 min. Propagation of optical action potentials was

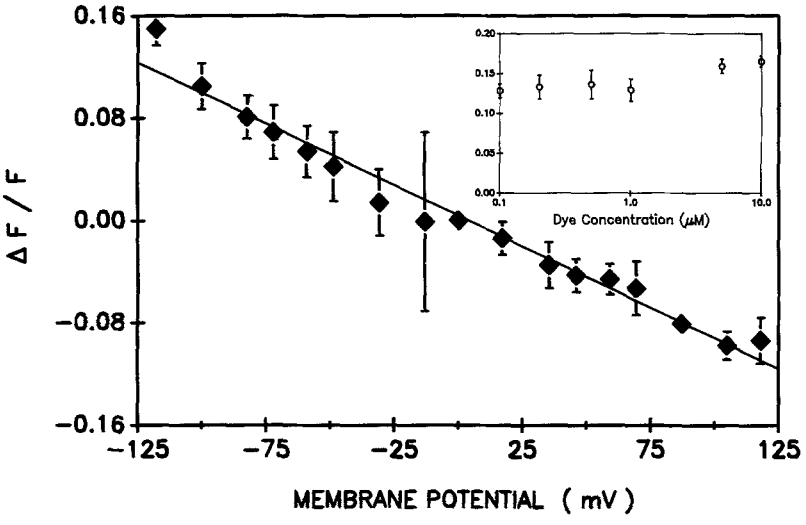

Fig. 5. Fractional fluorescence change as a function of membrane potential in lipid vesicles stained with di-4-ANEPPS. Lipid vesicles suspensions were prepared as in Fig. 3 using varying proportions of internal and external potassium to set the diffusion potentials. Excitation and emission wavelengths were set at 530 and 610 nm, respectively, corresponding to the maxima in the response spectra (Fig. 4). Each point is the average of at least six separate experiments from different vesicle preparations. The line through the points is the least squares fit with a slope of 9.6%/100 mV. The inset shows that the relative fluorescence change induced by a −120 mV potential is insensitive to the dye concentration between 0.1 and 10 μM.

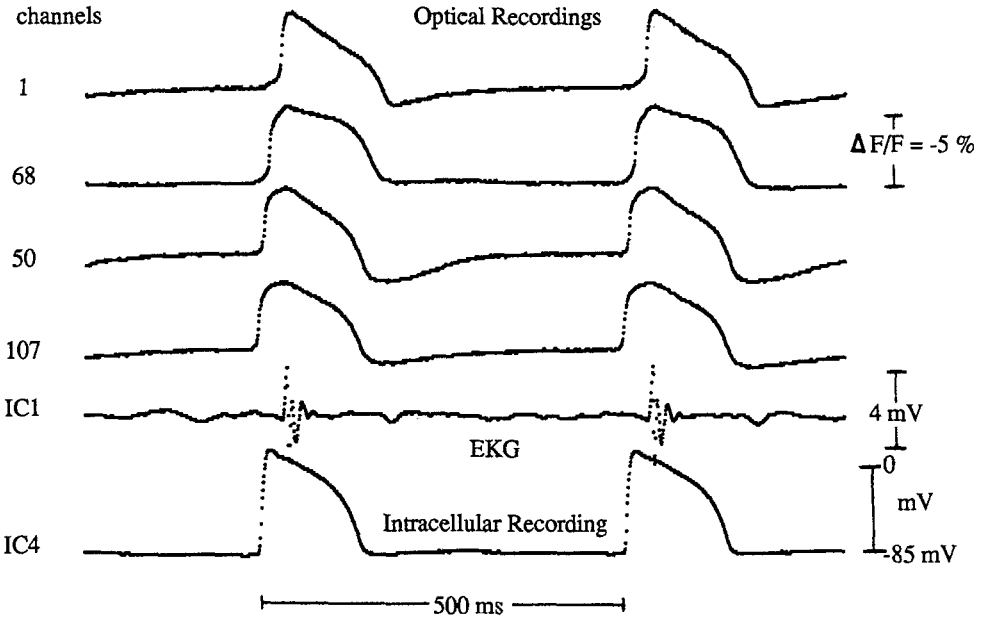

Fig. 6. Simultaneous recording of EKG, optical and microelectrode action potentials from guinea pig right ventricle. A Langendorff perfused guinea pig heart was stained with 10 μM di-4-ANEPPS for 5 min, the left ventricular free wall and septum were dissected and the perfused right ventricular sheet was pinned down horizontally in a Sylguard-coated chamber. A 12 × 12 mm region of perfused, right ventricular free wall was imaged on the photodiode array. The apex was electrically stimulated at 2 Hz with bipolar Ag/AgCl wires (100 μm, 0.5 mm apart). Two cycles of action potentials (1 kHz frequency response) are shown for diodes nos. 1, 68, 50, and 107 plus an EKG signal (recorded from the base of the ventricle; *see* Fig. 7) and a microelectrode impalement in a cell viewed by diode no. 50. The relative location of these recordings is identified in Fig. 7. The dye exhibited on average a 5.13 ± 0.2% decrease in fluorescence per action potential.

anisotropic with stable conduction velocities of 0.85 ± 0.12 and 0.44 ± .11 m/sec (n = 12) respectively, along the longitudinal and transverse axis of the fibers. Thus, di-4-ANEPPS stained guinea pig hearts reliably and homogeneously and yielded persistent optical action potentials with no indication of toxic effects on the ventricles.

Red Cells

The dye response to a valinomycin mediated K^+ diffusion potential in human red cells is shown in Fig. 8. As in the case of lipid vesicle suspensions, hyperpolarization induces an increase in fluorescence intensity superimposed on a bathochromic

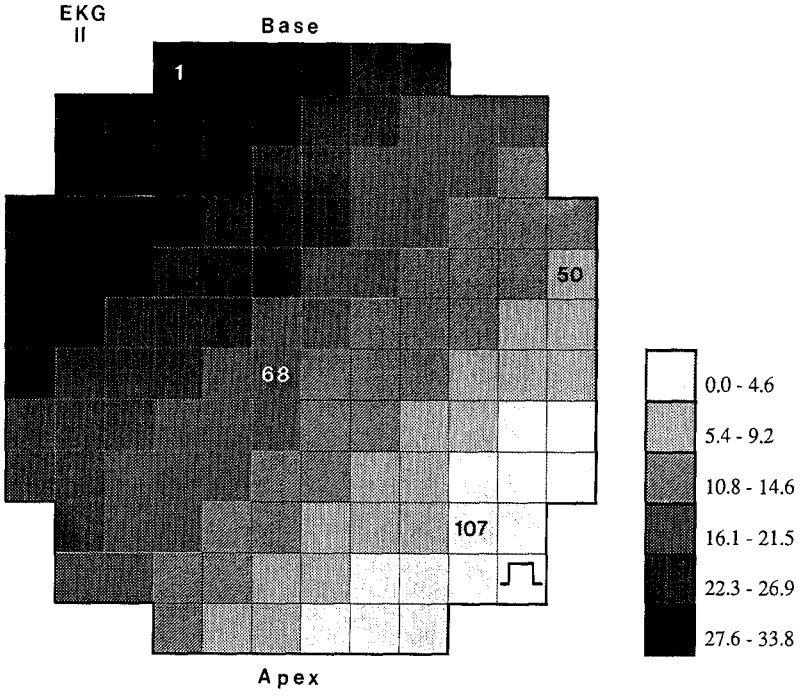

Fig. 7. Pattern of electrical activation in guinea pig ventricle. The time point, at which most of the cells viewed by a pixel fired, was determined from the maximum rate of rise of the optical action potential at the pixel. The grayscale shown in the lower right of the figure was used to translate these times into a pattern of activation displayed as an isochrone. The stimulus site is located at the apex and imaged onto the indicated diode in the lower right.

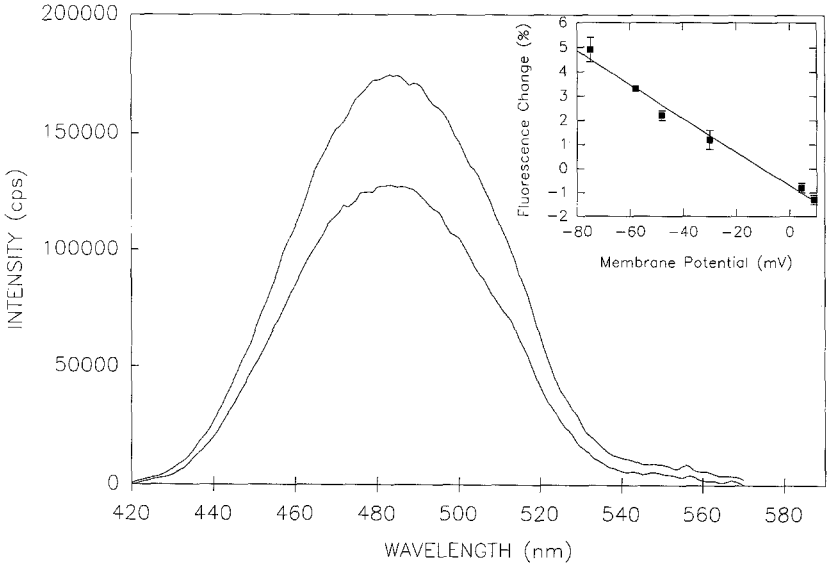

Fig. 8. Excitation spectra of di-4-ANEPPS in intact red cells before (lower) and after (upper) addition of valinomycin. Conditions: 1 μM dye; 0.05% hematocrit; 5 mM K^+; emission 610 nm. The inset shows a calibration obtained by varying the external [K^+] and dwelling at excitation and emission wavelengths of 492 and 630 nm, respectively.

wavelength shift. The calibration of the voltage-dependent fluorescence change is shown in the inset to Fig. 8. The change is linear with a slope of 7%/100 mV. Note that this calibration was performed at excitation and emission wavelengths of 492 and 630 nm, respectively; these correspond to the maxima in the difference between the pre- and post-valinomycin spectra, not the maxima in the *fractional* fluorescence response as in the lipid vesicle experiment (Fig. 5). Wavelengths at the blue and red wings of the excitation and emission spectra, respectively, would lead to more voltage sensitivity at the expense of overall fluorescence signal (i.e., signal-to-noise ratio).

The calibration in Fig. 8 is not very consistent. The amount of fluorescence enhancement (as opposed to wavelength shift) strongly depends on the dye : hematocrit ratio, the age of the red cells and the amount of valinomycin employed. In order to reduce this variability, we employed the dual wavelength approach introduced by Montana et al. (1989) for lipid vesicles and HeLa cells. Briefly, by using the ratio of fluorescence excited at wavelengths on the wings of the dye absorbance spectrum, contribu-

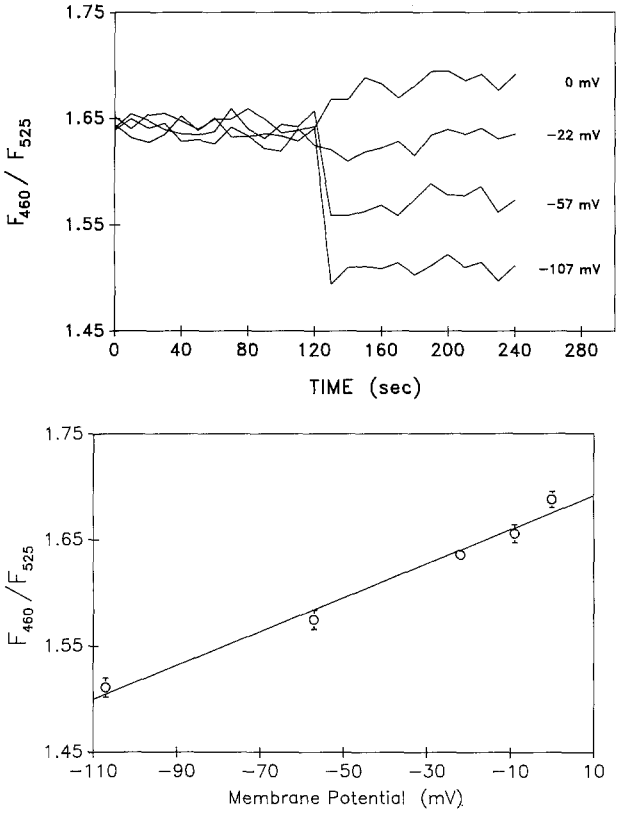

Fig. 9. Response to membrane potential of the ratio of fluorescence excited at 460 nm to that excited at 525 nm. Emission was set to 610 nm. Top panel: four kinetic traces obtained with varying external potassium concentrations; valinomycin was added at 120 sec in each experiment. Bottom panel: calibration of fluorescence ratio with membrane potential.

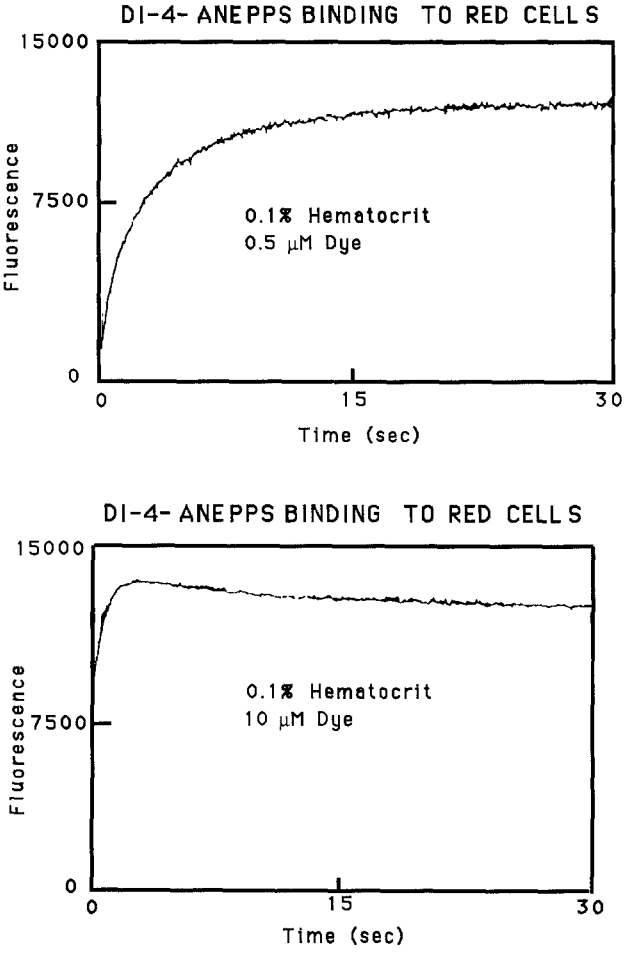

Fig. 10. Stopped-flow kinetics of di-4-ANEPPS binding to red cells. Excitation = 480 nm; emission > 590 nm. Top: equal volumes of 0.1% hematocrit red cell suspension and 0.5 μM dye were mixed at time 0. Bottom: equal volumes of 0.1% hematocrit and 10μM dye were mixed at time 0.

tions from fluctuations in overall dye intensity are normalized. This is particularly useful in experiments with relatively long durations where the level of dye binding or dye bleaching may change. Figure 9 shows that this approach can be used with good sensitivity; the slope of the fluorescence intensity ratio vs. membrane potential is 0.16/100 mV (although this calibration is dependent on the optical parameters set for the ratiometric spectrometer, the relative change in ratio should be dependent only on the choice of wavelengths). The data is Fig. 9 provide a value for the resting level corresponding to a membrane potential of *ca.* −13 mV; this is within the range of values obtained by other experimental approaches (Freedman & Laris, 1981).

To learn more about the probe response in red cells, we studied the kinetics of probe binding. Binding of the probe to a lipid bilayer leads to a large increase in fluorescence intensity (Fluhler et al., 1985) so the fluorescence could be used to monitor the rate of binding (Lojewska & Loew, 1987). Interestingly, the fluorescence change for binding to a red cell membrane cannot be fit to a single exponential function; at high concentrations, in fact, the dye fluorescence begins to decrease after an initial rapid rise. Kinetic curves for low and high dye concentrations are displayed in Fig. 10. These results require that binding must involve at least two distinct processes; the second slower process appears to be concentration dependent. Furthermore, similar behavior has been observed in kinetic experiments with red cell ghosts (Fluhler, 1987), suggesting that hemoglobin-mediated quenching following probe flipping cannot be an explanation for these results. High concentrations of dye tend to aggregate and produce broadened absorption spectra with quenched fluorescence, providing a rationale for the complex kinetics of Fig. 10. The involvement of a voltage-dependent dye aggregation, as has been observed with other potentiometric probes (Ross et

al., 1977; Waggoner et al., 1977; Dragsten & Webb, 1978), could help explain the intensity change which accompanies the wavelength shift of the voltage response in red cells.

Discussion

By examining the ability of di-4-ANEPPS to monitor membrane potential in several very different preparations, we hope to provide starting points for the establishment of protocols in other related situations for this versatile potentiometric indicator. In addition to the 4 systems examined here, reports have appeared in which di-4-ANEPPS has been applied to: (i) voltage-clamped spherical bilayers (Fluhler et al., 1985), (ii) external electric-field induced membrane potentials on A431 cells, RBL cells, rye protoplasts (Gross et al., 1986*b*) and HeLa cells (Ehrenberg et al., 1987), (iii) rat (Müller et al., 1989), guinea pig (Rosenbaum et al., 1991) and dog (Davidenko et al., 1992) cardiac muscle, and (iv) rat cervical ganglion microcultures (Chien & Pine, 1991). In all but the last case, the relative fluorescence change was in the range of 7–10%/100 mV. (In the sympathetic neuron microculture system, where the fluorescence change was 1%/100 mV, wavelengths were not optimized and background fluorescence was not subtracted.) Ross and Reichardt (1979) were the first to point out that dyes identified in the squid axon screening program might give small or totally different voltage-dependent optical signals in other preparations. Such variability has been the rule rather than the exception and has been described for some styryl dyes (Loew et al., 1985). Thus, the consistency of di-4-ANEPPS is striking and this, along with the low toxicity and persistence demonstrated in the guinea pig heart, helps recommend it as a good initial choice during the dye screening phase of projects requiring fast potentiometric indicators.

It is important to consider, however, the variability in the details of the behavior of di-4-ANEPPS. The changes in response to a potential step on the spherical bilayer can be interpreted exclusively in terms of a wavelength shift in both the absorbance and emission spectra (Fluhler et al., 1985). The excitation wavelength dependence of the fluorescence response in both the lipid vesicles (Fig. 3) and red cells (Fig. 8) indicate an overall change in fluorescence intensity superimposed on a wavelength shift. Often, the wavelength shift is masked by the large intensity change and only becomes apparent in difference spectra or dual-wavelength ratios. The sensitivity of the dye is dependent on concentration in red cells, where it also displays complex binding kinetics (Fig. 10), but not in lipid vesicles. The relative fluorescence change on the squid axon is much lower than in the other systems, presumably due to high fluorescence from glial cells in the preparation. Clearly, it is necessary to thoroughly investigate the behavior of the dye in any new preparation before using it as a monitor of membrane potential.

As demonstrated here for red cells (Fig. 9) and earlier for lipid vesicles and HeLa cells (Montana et al., 1989), the dye can be used in a dual wavelength ratiometric mode to measure membrane potential. This relies on the potential-dependent wavelength shift of the excitation spectrum—probably an invariant but not exclusive component of the dye response. This mode adds another level of usefulness to the dye because it permits monitoring of long-term potential changes where dye bleaching or removal during perfusion changes the absolute level of fluorescence but not the dual- wavelength ratio (Jesurum & Gross, 1991). It also obviates single cell measurements of potential variation along the cell surface by dual wavelength imaging (Ehrenberg, Wei & Loew, 1990); variable staining along the irregular membrane of most cells precludes single wavelength measurements.

There are situations in which some of the physical-chemical properties of di-4-ANEPPS are not optimal. It has been reported that there are a number of cultured cell lines in which di-4-ANEPPS rapidly internalizes upon application (Gross et al., 1986*b*; Gross & Loew, 1989). Staining of the inner leaflet of the plasma membrane or the membranes of internal organelles will produce, respectively, an opposing voltage-dependent response or large background fluorescence. Dye flipping can be retarded by increasing the chain length of the alkyl groups appended to the dye chromophore, and we have synthesized such a compound—di-8-ANEPPS (Ehrenberg et al., 1990). On the other hand, di-4-ANEPPS is not sufficiently water soluble for experiments requiring microinjection to localize stain to one cell in a complex preparation. We have synthesized dyes with shorter chains and more polar head groups appended to the ANEP chromophore. These compounds should have the appropriate solubility characteristics for use as intracellular probes while preserving the good sensitivity and versatility of di-4-ANEPPS.

The authors are pleased to acknowledge the support of the U.S. Public Health Service grants GM35063, RR04139 and NS08437. Support from the American Heart Association (871065) and the Whitaker Foundation is also gratefully acknowledged. The detailed comments of a reviewer were most helpful in the preparation of a final version of the manuscript.

References

Chien, C.-B., Pine, J. 1991. Voltage-sensitive dye recording of action potentials and synaptic potentials from sympathetic microcultures. *Biophys. J.* **60:**697–711

Cohen, L.B., Salzberg, B.M., Davila, H.V., Ross, W.N., Landowne, D., Waggoner, A.S., Wang, C.H. 1974. Changes in axon fluorescence during activity: Molecular probes of membrane potential. *J. Membrane Biol.* **19:**1–36

Davidenko, J.M., Pertsov, A.V., Salomonsz, R., Baxter, W., Jalife, J. 1992. Stationary and drifting spiral waves of excitation in isolated cardiac muscle. *Nature* **355:**349–351

Davila, H.V., Cohen, L.B., Salzberg, B.M., Shrivastav, B.B. 1974. Changes in ANS and TNS fluorescence in giant axons from *Loligo*. *J. Membrane Biol.* **15:**29–46

Dragsten, P.R., Webb, W.W. 1978. Mechanism of the membrane potential sensitivity of the fluorescent membrane probe merocyanine 540. *Biochemistry* **17:**5228–5240

Ehrenberg, B., Farkas, D.L., Fluhler, E.N., Lojewska, Z., Loew, L.M. 1987. Membrane potential induced by external electric field pulses can be followed with a potentiometric dye. *Biophys. J.* **51:**833–837

Ehrenberg, B., Wei, M., Loew, L.M. 1990. Second order effects in the interaction of electric fields with cell membranes. *Biophys. J.* **57:**484*a*

Fluhler, E., Burnham, V.G., Loew, L.M. 1985. Spectra, membrane binding and potentiometric responses of new charge shift probes. *Biochemistry* **24:**5749–5755

Fluhler, E.N. 1987. *Characterization of new spectroscopic molecular probes of membrane potential.* Ph.D. Thesis. SUNY at Binghamton

Freedman, J.C., Laris, P.C. 1981. Electrophysiology of cells and organelles: Studies with optical potentiometric indicators. *In:* International Review of Cytology, Supplement 12, pp. 177–246. Academic, New York

Grinvald, A., Fine, A., Farber, I.C., Hildesheim, R. 1983. Fluorescence monitoring of electrical responses from small neurons and their processes. *Biophys. J.* **42:**195–198

Grinvald A.S., Hildesheim, R., Farber, I.C., Arglister, J. 1982. Improved fluorescent probes for the measurement of rapid changes in membrane potential. *Biophys. J.* **39:**301–308

Gross, D., Loew, L.M. 1989. Fluorescent indicators of membrane potential: Microspectrofluorometry and imaging. *In:* Methods in Cell Biology. Y. Wang and D.L. Taylor, editors. Vol. 30, pp. 193–218. Academic, New York

Gross, D., Loew, L.M., Ryan, T.A., Webb, W.W. 1986*a*. Spatially resolved optical imaging of membrane potentials induced by applied electric fields. *In:* Ionic Currents in Development. R. Nuccitelli, editor, pp. 263–270. Alan R. Liss, New York

Gross, D., Loew, L.M., Webb, W.W. 1986*b*. Optical imaging of cell membrane potential. Changes induced by applied electric fields. *Biophys. J.* **50:**339–348

Gupta, R.K., Salzberg, B.M., Grinvald, A., Cohen, L.B., Kamino, K., Lesher, S., Boyle, M.B., Waggoner, A.S., Wang, C.H. 1981. Improvements in optical methods for measuring rapid changes in membrane potential. *J. Membrane Biol.* **58:**123–137

Hassner, A., Birnbaum, D., Loew, L.M. 1984. Charge-shift probes of membrane potential synthesis. *J. Org. Chem.* **49:**2546–2551

Jesurum, A., Gross, D.J. 1991. Di-8-ANEPPS fluorescence imaging of membrane potential changes in individual EGF-stimulated A431 cells: novel kinetics and calcium dependence. *Biophys. J.* **59:**526*a*

Loew, L.M. 1988. Spectroscopic Membrane Probes. CRC, Boca Raton, (FL)

Loew, L.M., Simpson, L. 1981. Charge shift probes of membrane potential. A probable electrochromic mechanism for ASP probes on a hemispherical lipid bilayer. *Biophys. J.* **34:**353–365

Loew, L.M., Bonneville, G.W., Surow, J. 1978. Charge shift optical probes of membrane potential. Theory. *Biochemistry* **17:**4065–4071

Loew, L.M., Scully, S., Simpson, L., Waggoner, A.S. 1979. Evidence for a charge-shift electrochromic mechanism in a probe of membrane potential. *Nature* **281:**497–499

Loew, L.M., Cohen, .L.B., Salzberg, B.M., Obaid, A.L., Bezanilla, F. 1985. Charge shift probes of membrane potential. Characterization of aminostyrylpyridinium dyes on the squid giant axon. *Biophys. J.* **47:**71–77

Lojewska, Z., Loew, L.M. 1987. Insertion of amphiphilic molecules into membranes is catalyzed by a high molecular weight non-ionic surfactant. *Biochim. Biophys. Acta* **899:**104–112

Montana, V., Farkas, D.L., Loew, L.M. 1989. Dual wavelength ratiometric fluorescence measurements of membrane potential. *Biochemistry* **28:**4536–4539

Müller, W., Windisch, H., Tritthart, H.A. 1989. Fast optical monitoring of microscopic excitation patterns in cardiac muscle. *Biophys. J.* **56:**623–629

Platt, J.R. 1956. Electrochromism, a possible change of color producible in dyes by an electric field. *J. Chem. Phys.* **25:**80–105

Rosenbaum, D.S., Kaplan, D.T., Kanai, A., Jackson, L., Garan, H., Cohen, R.J., Salama, G. 1991. Repolarization inhomogeneities in ventricular myocardium change dynamically with abrupt cycle length shortening. *Circulation* **84:**1333–1345

Ross, W.N., Reichardt, L.F. 1979. Species-specific effects on the optical signals of voltage-sensitive dyes. *J. Membrane Biol.* **48:**343–356

Ross, W.N., Salzberg, B.M., Cohen, L.B., Grinvald, A., Davila, H.V., Waggoner, A.S., Wang, C.H. 1977. Changes in absorption, fluorescence, dichroism, and birefringence in stained giant axons: Optical measurement of membrane potential. *J. Membrane Biol.* **33:**141–183

Salama, G., Lombardi, R., Elson, J. 1987. Maps of optical action potentials and NADH fluorescence in intact working hearts. *J. Am. Physiol. Soc.* h384–h394

Waggoner, A.S., Wang, C.H., Tolles, R.L. 1977. Mechanism of potential-dependent light absorption changes of lipid bilayer membranes in the presence of cyanine and oxonol dyes. *J. Membrane Biol.* **33:**109–140

Received 3 December 1991; revised 29 April 1992